CHEMISTRY

Manipulation of an electron by photoirradiation in the electron-catalyzed cross-coupling reaction

Eiji Shirakawa[1]*, Yuki Ota[1], Kyohei Yonekura[1], Keisho Okura[1], Sahiro Mizusawa[1,2], Sujan Kumar Sarkar[3,4], Manabu Abe[3]*

An electron has recently been shown to catalyze the cross-coupling reaction of organometallic compounds with aryl halides. In terms of green and sustainable chemistry, the electron catalysis is much more desirable than the inevitably used transition metal catalysis but a high temperature of more than 100°C is required to achieve it. Here, we disclose that visible light photoirradiation accelerates the electron-catalyzed reaction of arylzinc reagents with aryl halides with the aid of a photoredox catalysis. Photoexcitation of a photoredox catalyst and an anion radical intermediate respectively affects the supply and transfer of the electron catalyst, promoting the cross-coupling reaction to proceed at room temperature. The supply of the electron catalyst by the photoredox catalysis makes the scope of aryl halides wider.

INTRODUCTION

Transition metal–catalyzed cross-coupling reactions of organometallic compounds with organic halides have been widely used in organic synthesis (*1*, *2*). Among these, the palladium-catalyzed cross-coupling reaction of arylmetals with aryl halides provides an indispensable method to prepare biaryl frameworks, which often appear in medicines and electric materials such as liquid crystals (*3*–*5*). In 2012, we reported the first electron-catalyzed cross-coupling reaction, which uses aryl Grignard reagents and aryl halides to obtain biaryls with no aid of a transition metal catalysis (*6*). The electron catalysis (*7*) has been further applied to the cross-coupling reaction of various organometallic reagents with aryl/alkenyl halides (*8*–*21*). As shown in Fig. 1, an electron catalyst is provided from an organometallic reagent (exemplified by an arylzinc halide, Ar^1–ZnX), through single-electron transfer (SET) toward an aryl halide (X–Ar^2) (step *a*). The resulting anion radical ([X–Ar^2]$^{\bullet -}$) undergoes carbon—carbon bond formation to be converted to anion radical [Ar^1–Ar^2]$^{\bullet -}$ (step *b*), which passes an electron to X–Ar^2 to close the electron catalytic cycle, giving the coupling product (Ar^1–Ar^2) and regenerating [X–Ar^2]$^{\bullet -}$ (step *c*). Here, SET in step *a* is considered to be reluctant, and thus, high temperatures of more than 100°C are required for the electron-catalyzed cross-coupling reactions to proceed. On the other hand, photoredox catalysis is efficiently used for the reduction of aryl halides (X–Ar^2) into arenes (H–Ar^2) (*22*, *23*). SET from an excited photoredox catalyst toward an aryl halide (X–Ar^2) gives anion radical [X–Ar^2]$^{\bullet -}$, which undergoes decomposition into the aryl radical and X^-, and the aryl radical is converted to the arene (H–Ar^2) through hydrogen atom abstraction. We anticipated that the incorporation of such a photoredox catalysis supplying an electron catalyst as a form of anion radical [X–Ar^2]$^{\bullet -}$ into the electron catalysis accelerates the cross-coupling reaction. The anticipation came true, and furthermore, photoirradiation was found to enhance the turnover of the electron catalytic cycle. Here, we report that the electron-catalyzed cross-coupling reaction of arylzinc reagents with aryl halides is accelerated by photoirradiation, which works in two different events: making a photoredox catalyst excited to work as an electron catalyst distributer (step *d*) and photoexciting anion radical [Ar^1–Ar^2]$^{\bullet -}$ of the coupling product (step *e*) to facilitate SET of the electron catalyst to the aryl halide.

RESULTS AND DISCUSSION

Introduction of a photoredox catalysis into the electron catalysis

The reaction of a phenylzinc reagent, prepared from phenylmagnesium bromide (**1a**: 1.4 equiv) and zinc chloride (1.5 equiv), with 3,5-xylyl iodide (**2a**, 0.10 M) in a 1:1 mixture of tetrahydrofuran (THF) and *N*,*N*-dimethylacetamide (DMA) at 25°C for 6 hours gave just 1% of the cross-coupling product (**3aa**: 3,5-dimethylbiphenyl) with 2% conversion of **2a** (entry 1 of Fig. 2). Even at an elevated temperature (110°C), the reaction is slow to require 24 hours to

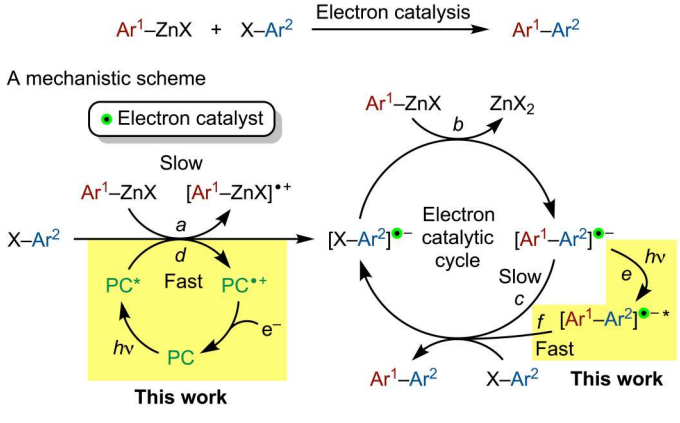

Fig. 1. The mechanism of the electron-catalyzed cross-coupling reaction and the photoacceleration disclosed in this work.

[1]Department of Applied Chemistry for Environment, School of Biological and Environmental Sciences, Kwansei Gakuin University, Sanda, Hyogo 669-1337, Japan. [2]Fine Materials Department, Osaka Gas Chemicals, Co., Ltd., Konohana-ku, Osaka, 554-0051, Japan. [3]Department of Chemistry, Graduate School of Advanced Science and Engineering, Hiroshima University, Higashihiroshima, Hiroshima 739-8526, Japan. [4]Advanced Patterning Department, Interuniversity Microelectronics Centre (IMEC), Leuven 3001, Belgium.
*Corresponding author. Email: eshirakawa@kwansei.ac.jp (E.S.); mabe@hiroshima-u.ac.jp (M.A.)

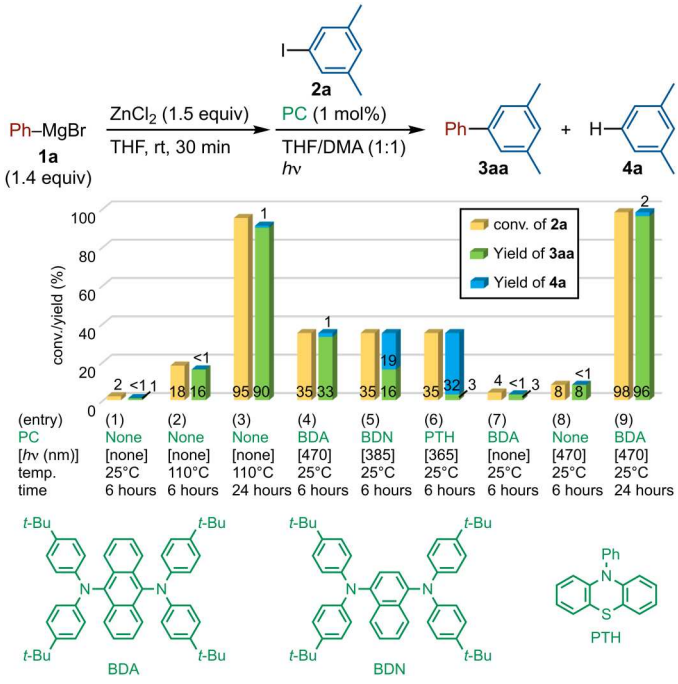

Fig. 2. Effect of photoredox catalysts in the reaction of a phenylzinc reagent with 3,5-xylyl iodide. The reaction was carried out under nitrogen atmosphere at 25° or 110°C for 6 or 24 hours using PhMgBr (**1a**: 0.56 mmol in 0.6 ml of THF), $ZnCl_2$ (0.60 mmol in 1.4 ml of THF), 3,5-xylyl iodide (**2a**: 0.40 mmol), a photoredox catalyst (PC; 0 or 4.0 μmol), DMA (2.0 ml), and an light-emitting diode (LED) lamp (0.60 W). Conversions (conv.) and yields were determined by gas chromatography based on **2a**.

reach a high conversion (entries 2 and 3). The effect of organic photoredox catalysts [1 mole percent (mol %)] was examined in the reaction at 25°C for 6 hours in combination with photoirradiation of an appropriate wavelength (entries 4 to 6). Among the examined catalysts, 9,10-bis[di(*p*-*tert*-butylphenyl)amino]anthracene (BDA) (*24*) was found to be the most effective to give **3aa** in 33% yield with 35% conversion of **2a** (entry 4). The use of BDN (*25*, *26*) or 10-phenylphenothiazine (PTH) (*22*) promoted the conversion of **2a** but the reduction into the arene (1,3-xylene: **4a**) predominates over the cross-coupling (entries 5 and 6). BDN and PTH (E^*_{ox} = −2.59 V and −2.85 V versus ferrocene, respectively), compared with BDA (E^*_{ox} = −2.03 V versus ferrocene), are known to have high reduction abilities upon photoexcitation. The use of BDA with no photoirradiation did not enhance the rate of the cross-coupling reaction, whereas the reaction was slightly promoted by photoirradiation in the absence of a photoredox catalyst (entries 7 and 8). By the use of BDA, the reaction at 25°C for 24 hours gave **3aa** in 96% yield (entry 9).

Expansion of the substrate scope

The cross-coupling reaction aided by the BDA photoredox catalysis is applicable to various combinations of arylzinc reagents and aryl halides at room temperature, though higher temperatures are required for high yields in some cases (Fig. 3). Aryl/heteroaryl iodides (**2**), bromides (**2′**), and chlorides (**2″**) having an electron-donating group or an electron-withdrawing group (EWG) reacted with the arylzinc reagents prepared through transmetalation between Ar^1MgBr and $ZnCl_2$ to give the corresponding coupling products in high yields (entries 1 to 59). This method features three advantages. The first advantage is the application to aryl chlorides, which are hard to accept a single-electron reduction. For instance, contrary to the idea that 1-chloro-4-(trifluoromethyl)benzene (**2″e**) was not converted at all even at high temperature (110°C) with no photoredox catalysis, the present method allows **2″e** to undergo coupling with the phenylzinc reagent to give 4-(trifluoromethyl)biphenyl (**3ae**) in 90% yield (entries 7 and 8). The trend was observed also in the reaction with 4-chloro-*N*,*N*-dimethylbenzamide (**2″f**) (entries 11 and 12) and 2-chloronaphthalene (**2″s**) (entries 35 and 36). The second advantage is functional group tolerance toward ketones and alkyl halides, which are damaged under high-temperature conditions (entries 13 to 15 and 20 and 21). The third advantage is the chemoselectivity concerning alkyne and alkene moieties in comparison with the palladium catalysis, which gives unsaturated bond-incorporated phenylation products in addition to the direct coupling product (entries 27 to 30). Preparation of arylzinc iodides (**1′**) from aryl iodides and zinc metal allows us to apply arylzincs having an EWG and 2-thienylzinc iodide (entries 60 to 65). The reaction of these arylzinc reagents was facilitated by the addition of $MgCl_2$ (4 equiv). *N*-Heteroaromatic substrates such as 3-iodopyridine, 3-bromopyridine, 6-iodoquinoline, and 3-pyridylzinc iodide are not applicable (see the Supplementary Materials).

Details of supply of the electron catalyst from the excited BDA

As clearly shown in Figs. 2 and 3, BDA plays a crucial role in accelerating the cross-coupling reaction under photoirradiation. To understand the role of BDA, the dynamic quenching experiments of its singlet and triplet excited states (^{1}[BDA]* and ^{3}[BDA]*) were conducted using fluorescence and transient absorption analyses (Fig. 4). Fluorescence emission decay was measured by a time-correlated single-photon counting method (*27*) to determine the lifetime ($^1\tau$) of ^{1}[BDA]* in THF/DMA (1:1) (fig. S4). The emission lifetime was found to be $^1\tau$ = ~31 ns ($1/^1\tau = {}^1k_d = 3.2 \times 10^7\ s^{-1}$) at ~298 K. The fluorescence lifetime of BDA was measured with different concentrations of ethyl 4-iodobenzoate (**2h**) (Fig. 4A). The fluorescence intensity and emission lifetime were quenched by increasing the concentration of **2h** ([**2h**]). All the lifetimes were obtained by fitting the decay using a monoexponential equation. From the slope of the Stern-Volmer plot, $^1\tau^0/^1\tau$ versus [**2h**], the rate constant (^1k_q) of the slow dynamic quenching of ^{1}[BDA]* by **2h** was determined to be $1.0 \times 10^7\ M^{-1}\ s^{-1}$. Next, to understand the reactivity of ^{3}[BDA]*, the laser flash photolysis experiments were conducted for the reaction with **2h** (Fig. 4B). The time profile monitored at 400 nm, which is the absorption maxima of the transient ultraviolet-visible spectrum (fig. S7), was fitted using a monoexponential equation to determine the lifetime ($^3\tau$) of 58.2 μs ($^3k_d = 1.7 \times 10^4\ s^{-1}$) at 293 K under argon atmosphere. The ^{3}[BDA]* lifetimes ($^3\tau$) were measured in the presence of **2h** to obtain the dynamic quenching rate constant (^3k_q) of ^{3}[BDA]* by **2h**. From the slope of the Stern-Volmer plot, $^3\tau^0/^3\tau$ versus [**2h**], the quenching rate constant, ^3k_q, was found to be $1.5 \times 10^5\ M^{-1}\ s^{-1}$. The dynamic quenching experiments clarified that both of ^{1}[BDA]* and ^{3}[BDA]* may react with **2h**. Because the singlet and triplet excited-state energies of BDA are lower than those of **2h** (figs. S8 and S9), the dynamic quenching mechanism is not the energy transfer reaction, but the electron

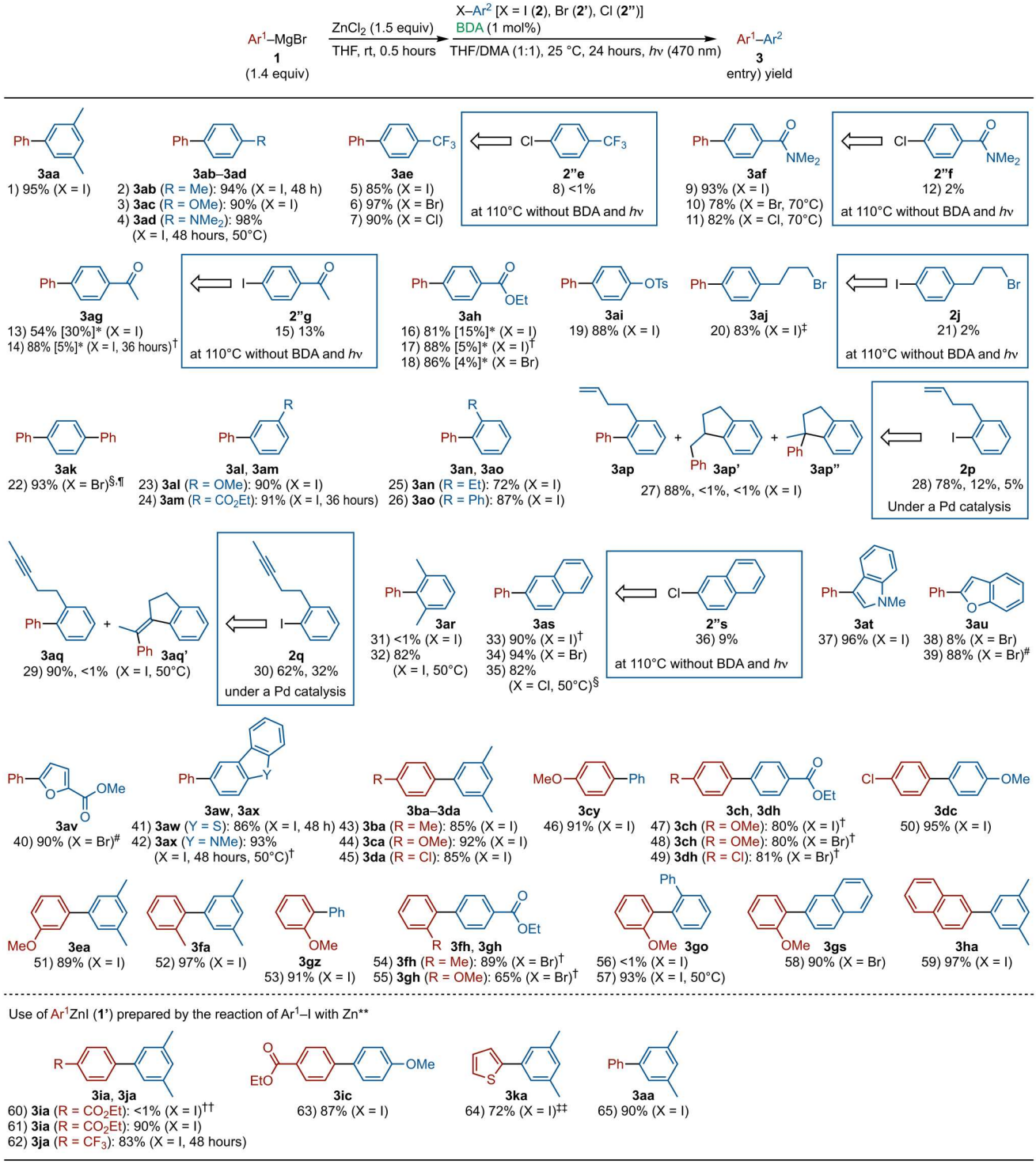

Fig. 3. Coupling of arylzinc reagents with aryl halides aided by the BDA photoredox catalysis. The reaction was carried out under nitrogen atmosphere at 25°C for 24 hours using an arylmagnesium bromide (**1**: 0.56 mmol in 0.6 ml of THF), $ZnCl_2$ (0.60 mmol in 1.4 ml of THF), an aryl halide (**2**, **2**′, or **2**″: 0.40 mmol), BDA (4.0 μmol), DMA (2.0 ml), and an LED lamp (λ_{max} = 470 nm, 0.60 W). The yield of the isolated product is based on **2**. *The yield of hydrodehalogenation products (**4**). †The radiated energy of the light is 0.03 W. ‡$ZnBr_2$ was used instead of $ZnCl_2$. §LiCl (0.60 mmol) was added. ¶1,4-Dibromobenzene (0.20 mmol) was used. #LiCl (1.6 mmol) was added. **An arylzinc iodide (**1**′: 0.56 mmol in THF/Tetramethylurea) with $MgCl_2$ (1.6 mmol) was used. ††Without $MgCl_2$. ‡‡**1**′**k** (1.12 mmol) was used in the presence of LiCl (1.6 mmol) instead of $MgCl_2$.

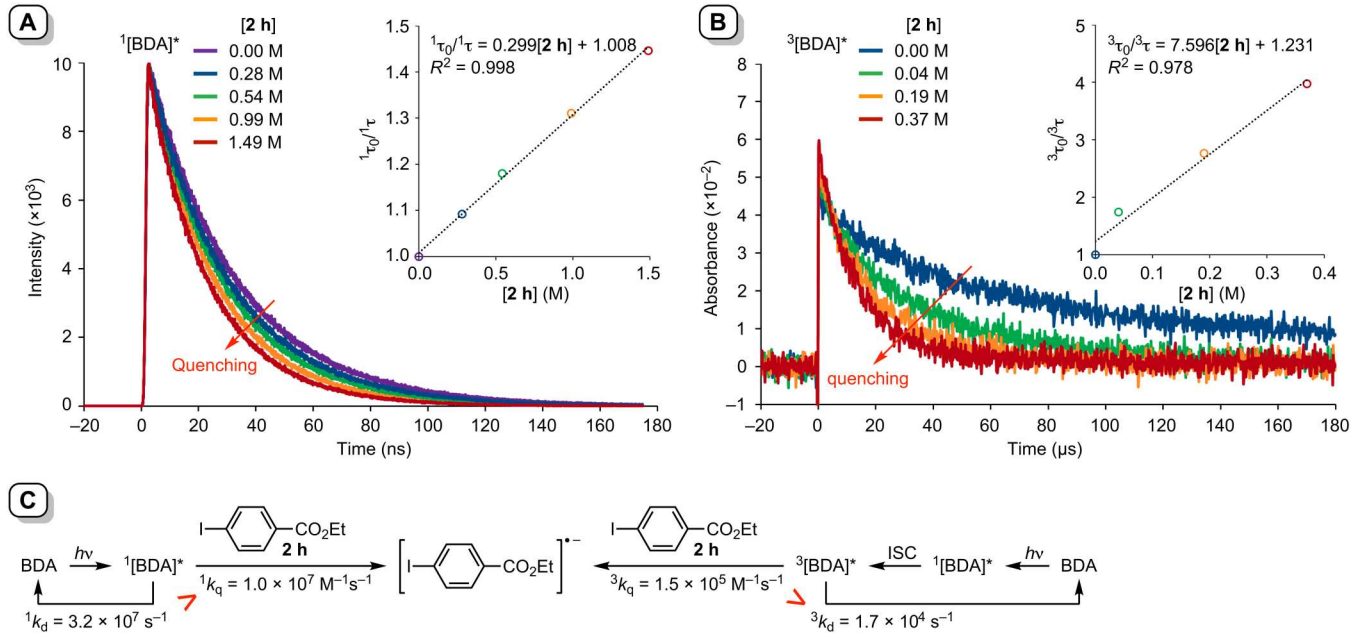

Fig. 4. Observation of single-electron transfer process from excited BDAs. (**A**) Fluorescence decay of BDA (0.01 mM) at 650 nm under nitrogen atmosphere in THF/DMA (1:1) in the presence of different amounts of **2h** ([**2h**] = 0, 0.28, 0.54, 0.99, 1.49 M) at a room temperature (excitation wavelength, 393 nm). Stern-Volmer plot obtained from fluorescence lifetimes at 650 nm in the presence of different concentrations of **2h**, where $^1\tau^0$ is the lifetime in absence of **2h** and $^1\tau$ is the lifetime at various concentrations of **2h**. (**B**) Time profile of ^{3}[BDA]* in THF/DMA (1:1) in the presence of **2h** ([**2h**] = 0, 0.04, 0.19, 0.37 M). The time profile is obtained from transient ultraviolet-visible spectra of 0.1 mM solution of BDA in THF/DMA (1:1) under a nitrogen atmosphere using 460 nm (optical parametric oscillator laser), 4 mJ. Stern-Volmer plot obtained from lifetimes observed at different concentration of **2h** at 400 nm, where $^3\tau^0$ is the lifetime in the absence of **2h**, and $^3\tau$ is the lifetime at various concentrations of **2h**. (**C**) A plausible mechanism.

transfer reaction (step *d* in Fig. 1). As judged by the quenching rate constants and the decay rate constants of ^{1}[BDA]* and ^{3}[BDA]*, ^{1}[BDA]* can be quenched only at the high concentration of **2h**, [**2h**] > 3 M, whereas ^{3}[BDA]* plays the important role in the reaction with **2h** (Fig. 4C).

Photoexcitation-induced transfer of the electron catalyst

Now, the BDA photoredox catalysis was found to be able to introduce electrons to catalyze the cross-coupling reaction at a low temperature such as room temperature. Here, once a sufficient number of electrons are introduced under photoirradiation in combination with BDA, the cross-coupling reaction should keep on going even after photoirradiation is ceased. Then, the progress of the reaction of the phenylzinc reagent with 2-bromonaphthalene (**2′s**) was tracked during repeated on-off sequences of photoirradiation (470 nm) (Fig. 5A). Contrary to our expectation, the reaction stopped when photoirradiation was ceased and revived when photoirradiation is restored. The result implies that photoirradiation has some effect on the electron catalytic cycle consisting of steps *b* and *c* in Fig. 1 besides the BDA photoredox catalysis in step *d* to provide an electron catalyst. The effect of photoirradiation on the electron catalytic cycle was confirmed by the cross-coupling reaction under photoirradiation in combination with a chemical injection of an electron catalyst in the absence of a photoredox catalyst (Fig. 5B) (*28*). Thus, 2-bromonaphthalene was first treated with sodium 2-methylnaphthalenide (2 mol %) for 10 min at room temperature and then with the phenylzinc reagent (1.4 equiv) at 25°C for 6 hours under irradiation of diverse wavelength. Contrary to the idea that the coupling product (2-phenylnaphthalene: **3as**) was hardly obtained in the dark, irradiation of light of wavelength ranging from 365 to 521 nm was found to promote the cross-coupling reaction, where the light of 365 nm is the most effective to give **3as** in 40% yield. The effect of wavelengths on the yield was found to have a strong correlation with the absorption spectrum of an anion radical ([**3as**]$^{\bullet -}$) of the coupling product, prepared through the reduction of **3as** by sodium, implying that photoirradiation affects the excitation of anion radicals of the coupling products. The outcome is rationally understood, considering that it promotes the electron transfer toward an aryl halide (Fig. 5C). However, the lifetime of excited states of anion radicals are generally known to be too short to pass the electron to another molecule (*29*–*36*). Then, the feasibility of the photoinduced SET was examined. Thus, [**3as**]$^{\bullet -}$, prepared from **3as** and sodium, was treated with 4-chloroanisole (**2″c**), which is one of the least reducible aryl halides, at −30°C for 5 min with or without photoirradiation to give anisole (**4a**) through SET from [**3as**]$^{\bullet -}$ to **1″c** followed by elimination of Cl^- and hydrogen abstraction (1 equiv) (Fig. 5D). Contrary to the idea that almost no **4c** was produced in the dark, the reduction was induced by photoirradiation at 365 to 631 nm to give **4c**. Here again, a strong correlation between the effect of wavelengths on the yield and the absorption spectrum of [**3as**]$^{\bullet -}$ was found, implying that the electron transfer from excited anion radicals of coupling products to aryl halides is feasible.

At the excitation wavelength of 470 nm, BDA emits yellow light as shown in Fig. 5E. The fluorescence quantum yield in THF/DMA is 65%. The fluorescence with λ_{em} 500 to 670 nm is strong even during the cross-coupling reaction with the aid of the BDA catalysis. It is natural that the electron catalytic cycle is affected by the

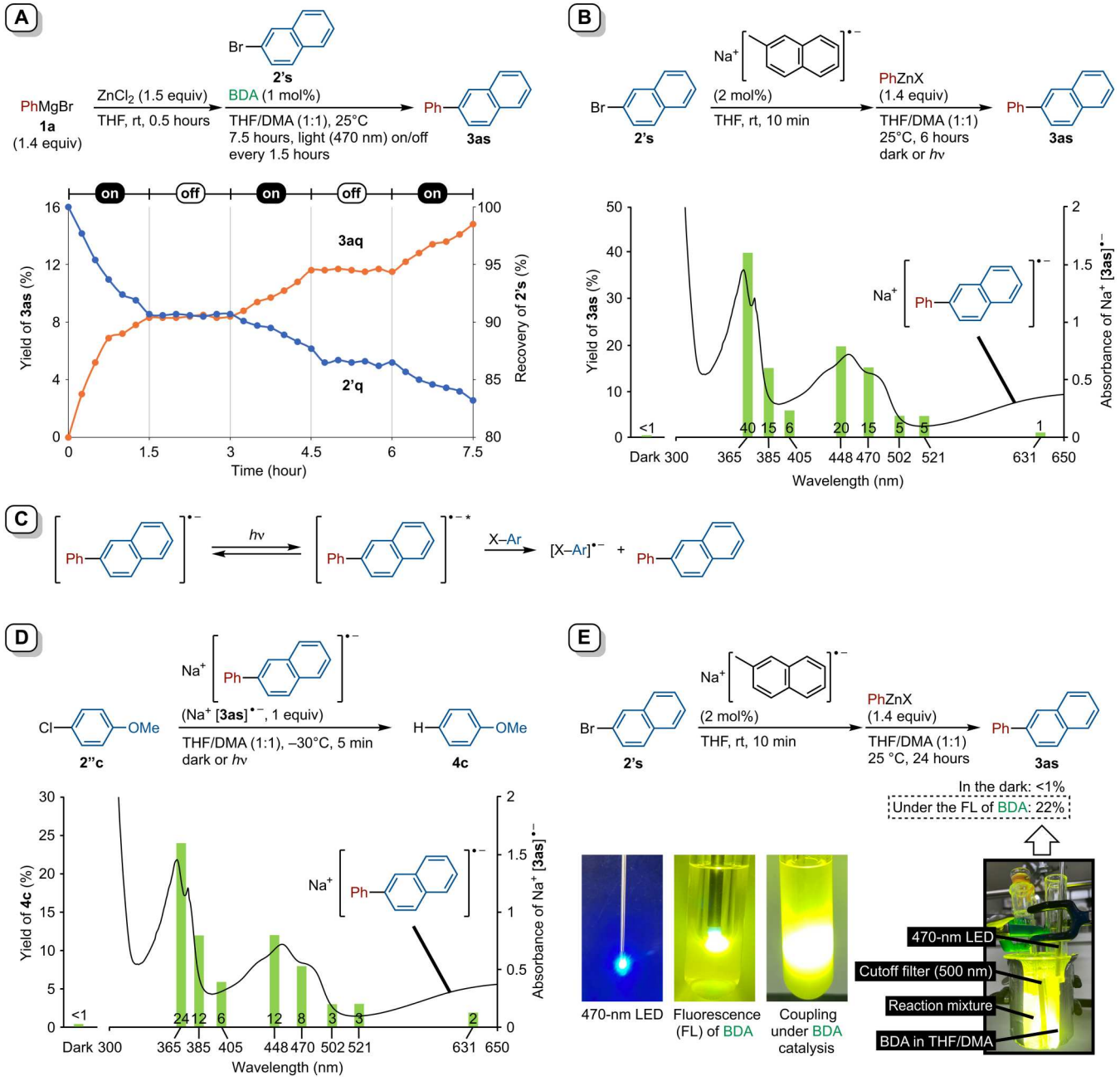

Fig. 5. Effect of light on single-electron transfer from an anion radical of a coupling product. (**A**) A "light/dark" experiment for the coupling of the phenylzinc reagent with 2-bromonaphthalene (**2′s**) aided by the BDA photoredox catalysis. (**B**) Comparison of the action spectrum for the coupling of the phenylzinc reagent with 2-bromonaphthalene (**2′s**) in the presence of sodium 2-methylnaphthalenide with the absorption spectrum (right axis) of [**3as**]$^{\bullet -}$ (1.0×10^{-3} M) in THF/DMA (1:1). The yield of the coupling product (**3as**) (left axis) versus the respective wavelengths of the reaction is shown. The reaction was carried out under photoirradiation (0.30 W). (**C**) Plausible reaction mechanism. (**D**) Comparison of the action spectrum for reduction of 4-chloroanisole (**1″c**) into anisole (**4c**) with sodium 2-phenylnaphthalenide (Na$^+$ [**3as**]$^{\bullet -}$) with the absorption spectrum (right axis) of [**3as**]$^{\bullet -}$ (1.0×10^{-3} M) in THF/DMA (1:1). The yield of the reduction product (**4c**) (left axis) versus the respective wavelengths of the reaction is shown. The reaction was carried out under photoirradiation (0.30 W). (**E**) The effect of the fluorescence of BDA on the coupling of the phenylzinc reagent with 2-bromonaphthalene (**2′s**) in the presence of sodium 2-methylnaphthalenide. Photos of a 470-nm LED lamp, the fluorescence of BDA excited by a 470-nm LED lamp, the coupling reaction under a BDA photoredox catalysis, and the coupling under the fluorescence of BDA are also put here.

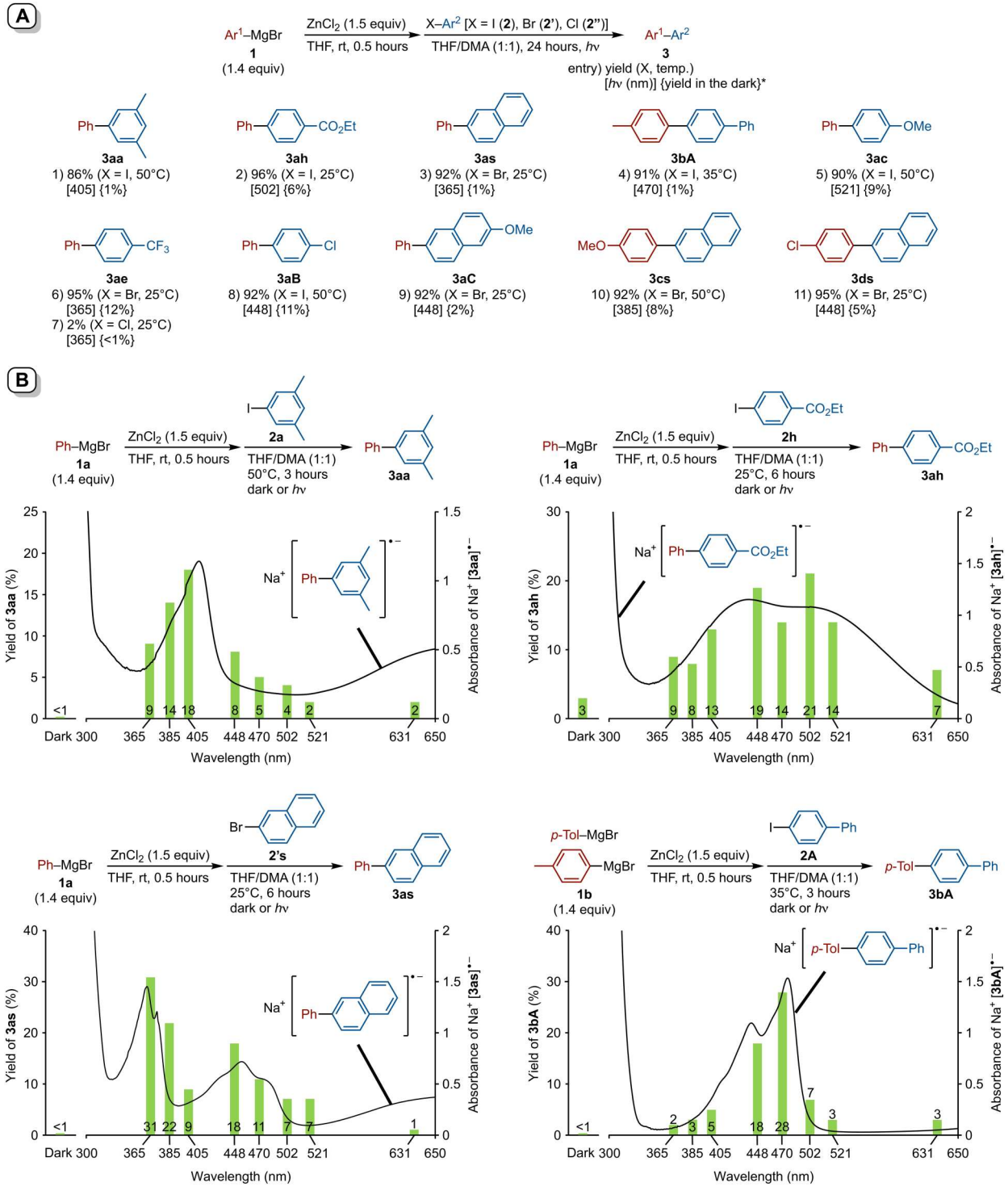

Fig. 6. Coupling of arylzinc reagents with aryl halides under photoirradiation. (**A**) The reaction was carried out under nitrogen atmosphere at 25°, 35°, or 50°C for 24 hours using an arylmagnesium bromide (**1**: 0.56 mmol in 0.6 ml of THF), $ZnCl_2$ (0.60 mmol in 1.4 ml of THF), an aryl halide (**2** or **2**′: 0.40 mmol), DMA (2.0 ml), and an LED lamp (λ_{max} = 470 nm, 8.4×10^{-7} einstein/s). The yield of the isolated product is based on **2**. The yield in the dark is shown in curly brackets. (**B**) Comparison of the action spectrum for the coupling of the arylzinc reagents with aryl halides in the absence of a photoredox catalyst with the absorption spectrum (right axis) of $[\mathbf{3}]^{\bullet -}$ (1.0×10^{-3} M) in THF/DMA (1:1). The yield of the coupling product (left axis) versus the respective wavelengths of the reaction is shown. The reaction was carried out under photoirradiation (8.4×10^{-7} einstein/s).

fluorescence, which is absorbed by the anion radical of 2-phenylnaphthalene ([**3as**]$^{\bullet -}$) to some extent. Then, the effect was confirmed by the coupling of 2-bromonaphthalene (**2′s**) with the phenylzinc reagent (1.4 equiv) in the presence of sodium 2-methylnaphthalenide (2 mol %) in the dark or under the fluorescence of BDA. Contrary to the idea that the coupling reaction in the dark did not proceed at all, the coupling product was obtained in 22% yield under the fluorescence of BDA but with cutting light of wavelength less than 500 nm with a cutoff glass filter (500 nm). These results exactly show that the fluorescence of BDA affects the electron catalytic cycle. Note that the BDA photoredox catalysis plays two roles, namely, the excited BDA supplies the electron catalyst and the fluorescence enhances the turnover of the electron catalytic cycle.

Reaction mechanism

On the basis of the above results and previous reports, a plausible mechanism for the photoinduced electron-catalyzed cross-coupling reaction is drawn as shown in Fig. 1. The trigger of the reaction is the excitation of BDA to give its singlet excited state (^{1}[BDA]*), which is transformed into its triplet excited state (^{3}[BDA]*) through the intersystem crossing. Electron transfer from ^{3}[BDA]* to an aryl halide (X–Ar^2) takes place to form anion radical [X–Ar^2]$^{\bullet -}$ and the cation radical of BDA (BDA$^{\bullet +}$) (step *d*), which is reduced by some species such as an arylzinc reagent (Ar^1–ZnX) to regenerate BDA. [X–Ar^2]$^{\bullet -}$ is converted to an anion radical ([Ar^1–Ar^2]$^{\bullet -}$) of the coupling product upon reaction with Ar^1–ZnX (step *b*). [Ar^1–Ar^2]$^{\bullet -}$ is excited by both the irradiated light (470 nm) and the fluorescence of BDA (step *e*) to [Ar^1–Ar^2]$^{\bullet -}$*, which pass an electron to X–Ar^2, giving the coupling product (Ar^1–Ar^2) and regenerating [X–Ar^2]$^{\bullet -}$ (step *f*) (see the Supplementary Materials for detailed discussion).

Application of manipulation of electron using light

Thus far, photoirradiation has been shown to accelerate the cross-coupling reaction by exciting both the BDA photoredox catalyst and anion radicals of the coupling products to affect respectively the supply and transfer of the electron catalyst. Thus, when the electron catalyst is provided in a small but sufficient amount from arylzinc reagents through SET to aryl halides (step *a* in Fig. 1), photoirradiation in the absence of any photoredox catalyst is expected to accelerate the cross-coupling reaction by exciting anion radicals of the coupling products, as the slight effect was already observed in entry 8 of Fig. 2. Actually, the coupling of arylzinc reagents with aryl halides was accelerated alone by irradiation of light of a wavelength ranging from 365 to 502 nm (Fig. 6A). An effective wavelength depends on the coupling product, being consistent with the consideration that the photoacceleration is brought about by the photoexcitation of anion radicals of the coupling products. The consideration was further confirmed by the observation that the effect of wavelengths on the yield of the cross-coupling reaction has a strong correlation with the absorption spectrum of an anion radical of the corresponding coupling product (Fig. 6B). As a matter of course, for the reaction of aryl halides, the reduction potentials of which are too negative and thus the supply of the electron catalyst through SET from arylzinc reagents to the aryl halides is insufficient, no acceleration was observed by photoirradiation as in the case with *p*-(trifluoromethyl)phenyl chloride (**2″e**) (entry 7 of Fig. 6A). For this aryl chloride, the assistance of the BDA photoredox catalysis is indispensable for the coupling reaction to take place (cf. entry 7 of Fig. 3).

In summary, we have developed the efficient electron-catalyzed cross-coupling reaction accelerated by photoirradiation with the aid of a BDA photoredox catalyst. The reaction is applicable to a wide range of aryl halides including less reducible aryl chlorides, which react with arylzinc reagents at a room temperature with high functional group tolerance. Mechanistic studies clarified that photoirradiation contributes to excitation of two species: the BDA photoredox catalyst to supply the electron catalyst and anion radicals of the coupling products to transfer the electron catalyst to aryl halides. Furthermore, the fluorescence of BDA was found to enhance the transfer of the electron catalyst. Photoirradiation alone in the absence of any photoredox catalyst accelerates the cross-coupling reaction of aryl halides having a relatively low LUMO energy level by promoting the transfer of the electron catalyst to enhance the turnover of the electron catalytic cycle.

MATERIALS AND METHODS

Representative procedure for the coupling of arylzinc reagents with aryl halides

To a partial suspension of $ZnCl_2$ (81.8 mg, 0.600 mmol) in THF (1.40 ml) in a 15-ml test tube equipped with a stir bar, a THF solution of phenylmagnesium bromide (**1a**, 0.93 M, 0.60 ml, 0.56 mmol) was added in a glove box, and the resulting mixture was stirred at a room temperature for 30 min. To the mixture was added successively with BDA (2.9 mg, 4.0 μmol), 3,5-xylyl iodide (**2a**: 92.8 mg, 0.400 mmol), and DMA (2.00 ml). The test tube was sealed with an inner glass tube to insert a light source and taken out of the glove box. The resulting mixture was stirred at 25°C for 24 hours under photoirradiation by a 470-nm light-emitting diode lamp cooled with blowing air. The reaction mixture was quenched with a saturated NH_4Cl aqueous solution (2 ml) and extracted with Et_2O (10 ml × 3). The combined organic layer was washed with water (10 ml × 3) and brine (10 ml). The organic layer was dried over $MgSO_4$, filtered, and concentrated in vacuo. The residue was subjected to silica gel chromatography (hexane, MPLC) to give 3,5-dimethylbiphenyl (**3aa**: 69.2 mg, 95% yield, entry 1 of Fig. 3).

Supplementary Materials

This PDF file includes:

Supplementary Materials and Methods
Supplementary Text
Figs. S1 to S27
References

REFERENCES AND NOTES

1. J. Hassan, M. Sévignon, C. Gozzi, E. Schulz, M. Lemaire, Aryl–aryl bond formation one century after the discovery of the Ullmann reaction. *Chem. Rev.* **102**, 1359–1470 (2002).
2. D. Haas, J. M. Hammann, R. Greiner, P. Knochel, Recent developments in Negishi cross-coupling reactions. *ACS Catal.* **6**, 1540–1552 (2016).
3. K. C. Nicolaou, P. G. Bulger, D. Sarlah, Palladium-catalyzed cross-coupling reactions in total synthesis. *Angew. Chem. Int. Ed.* **44**, 4442–4489 (2005).
4. J. Magano, J. R. Dunetz, Large-scale applications of transition metal-catalyzed couplings for the synthesis of pharmaceuticals. *Chem. Rev.* **111**, 2177–2250 (2011).
5. S. Huo, R. Mroz, J. Carroll, Negishi coupling in the synthesis of advanced electronic, optical, electrochemical, and magnetic materials. *Org. Chem. Front.* **2**, 416–445 (2015).

6. E. Shirakawa, Y. Hayashi, K. Itoh, R. Watabe, N. Uchiyama, W. Konagaya, S. Masui, T. Hayashi, Cross-coupling of aryl Grignard reagents with aryl iodides and bromides through $S_{RN}1$ pathway. *Angew. Chem. Int. Ed.* **51**, 218–221 (2012).
7. A. Studer, D. P. Curran, The electron is a catalyst. *Nat. Chem.* **6**, 765–773 (2014).
8. S. Murarka, A. Studer, Radical/anionic $S_{RN}1$-type polymerization for preparation of oligoarenes. *Angew. Chem. Int. Ed.* **51**, 12362–12366 (2012).
9. N. Uchiyama, E. Shirakawa, T. Hayashi, Single electron transfer-induced Grignard cross-coupling involving ion radicals as exclusive intermediates. *Chem. Commun.* **49**, 364–366 (2013).
10. E. Shirakawa, R. Watabe, T. Murakami, T. Hayashi, Single electron transfer-induced cross-coupling reaction of alkenyl halides with aryl Grignard reagents. *Chem. Commun.* **49**, 5219–5221 (2013).
11. H. Minami, X. Wang, C. Wang, M. Uchiyama, Direct C–C bond construction from arylzinc reagents and aryl halides without external catalysts. *Eur. J. Org. Chem.* **2013**, 7891–7894 (2013).
12. E. Shirakawa, F. Tamakuni, E. Kusano, N. Uchiyama, W. Konagaya, R. Watabe, T. Hayashi, Single-electron-transfer-induced coupling of arylzinc reagents with aryl and alkenyl halides. *Angew. Chem. Int. Ed.* **53**, 521–525 (2014).
13. B. E. Haines, O. Wiest, SET-induced biaryl cross-coupling: An $S_{RN}1$ reaction. *J. Org. Chem.* **79**, 2771–2774 (2014).
14. E. Shirakawa, K. Okura, N. Uchiyama, T. Murakami, T. Hayashi, Improved procedure for single-electron-transfer-induced Grignard cross-coupling reaction. *Chem. Lett.* **43**, 922–924 (2014).
15. H. Minami, T. Saito, C. Wang, M. Uchiyama, Organoaluminum-mediated direct cross-coupling reactions. *Angew. Chem. Int. Ed.* **54**, 4665–4668 (2015).
16. K. Okura, E. Shirakawa, Single-electron-transfer-induced coupling of alkylzinc reagents with aryl iodides. *Eur. J. Org. Chem.* **2016**, 3043–3046 (2016).
17. Q. He, L. Wang, Y. Liang, Z. Zhang, S. F. Wnuk, Transition-metal-free cross-coupling of aryl halides with arylstannanes. *J. Org. Chem.* **81**, 9422–9427 (2016).
18. K. Okura, H. Kawashima, F. Tamakuni, N. Nishida, E. Shirakawa, Single electron transfer-induced coupling of alkynylzinc reagents with aryl and alkenyl iodides. *Chem. Commun.* **52**, 14019–14022 (2016).
19. K. Kiriyama, K. Okura, F. Tamakuni, E. Shirakawa, Electron-catalyzed coupling of magnesium amides with aryl iodides. *Chem. A Eur. J.* **24**, 4519–4522 (2018).
20. K. Okura, T. Teranishi, Y. Yoshida, E. Shirakawa, Electron-catalyzed cross-coupling of arylboron compounds with aryl iodides. *Angew. Chem. Int. Ed.* **57**, 7186–7190 (2018).
21. E. F. Woods, A. J. Berl, J. A. Kalow, Photocontrolled synthesis of n-type conjugated polymers. *Angew. Chem. Int. Ed.* **59**, 6062–6067 (2020).
22. E. H. Discekici, N. J. Treat, S. O. Poelma, K. M. Mattson, Z. M. Hudson, Y. Luo, C. J. Hawker, J. Read de Alaniz, A highly reducing metal-free photoredox catalyst: Design and application in radical dehalogenations. *Chem. Commun.* **51**, 11705–11708 (2015).
23. R. Matsubara, T. Yabuta, U. Md Idros, M. Hayashi, F. Ema, Y. Kobori, K. Sakata, UVA- and visible-light-mediated generation of carbon radicals from organochlorides using nonmetal photocatalyst. *J. Org. Chem.* **83**, 9381–9390 (2018).
24. N. Noto, Y. Tanaka, T. Koike, M. Akita, Strongly reducing (diarylamino)anthracene catalyst for metal-free visible-light photocatalytic fluoroalkylation. *ACS Catal.* **8**, 9408–9419 (2018).
25. N. Noto, T. Koike, M. Akita, Visible-light-triggered monofluoromethylation of alkenes by strongly reducing 1,4-bis(diphenylamino)naphthalene photoredox catalysis. *ACS Catal.* **9**, 4382–4387 (2019).
26. N. Noto, K. Takahashi, S. Goryo, A. Takakado, K. Iwata, T. Koike, M. Akita, Laser flash photolysis studies on radical monofluoromethylation by (diarylamino)naphthalene photoredox catalysis: Long lifetime of the excited state is not always a requisite. *J. Org. Chem.* **85**, 13220–13227 (2020).
27. B. Valeur, M. N. Berberan-Santos, *Molecular Fluorescence: Principles and Applications* (Wiley-VCH, 2002).
28. I. M. Irshadeen, S. L. Walden, M. Wegener, V. X. Truong, H. Frisch, J. P. Blinco, C. Barner-Kowollik, Action plots in action: In-depth insights into photochemical reactivity. *J. Am. Chem. Soc.* **143**, 21113–21126 (2021).
29. M. Marchini, A. Gualandi, L. Mengozzi, P. Franchi, M. Lucarini, P. G. Cozzi, V. Balzani, P. Ceroni, Mechanistic insights into two-photon-driven photocatalysis in organic synthesis. *Phys. Chem. Chem. Phys.* **20**, 8071–8076 (2018).
30. M. Neumeier, D. Sampedro, M. Májek, V. A. de la Peña O'Shea, A. Jacobi von Wangelin, R. Pérez-Ruiz, Dichromatic photocatalytic substitutions of aryl halides with a small organic dye. *Chem. A Eur. J.* **24**, 105–108 (2018).
31. H. Kim, H. Kim, T. H. Lambert, S. Lin, Reductive electrophotocatalysis: Merging electricity and light to achieve extreme reduction potentials. *J. Am. Chem. Soc.* **142**, 2087–2092 (2020).
32. N. G. W. Cowper, C. P. Chernowsky, O. P. Williams, Z. K. Wickens, Potent reductants via electron-primed photoredox catalysis: Unlocking aryl chlorides for radical coupling. *J. Am. Chem. Soc.* **142**, 2093–2099 (2020).
33. I. A. MacKenzie, L. Wang, N. P. R. Onuska, O. F. Williams, K. Begam, A. M. Moran, B. D. Dunietz, D. A. Nicewicz, Discovery and characterization of an acridine radical photoreductant. *Nature* **580**, 76–80 (2020).
34. J. P. Cole, D.-F. Chen, M. Kudisch, R. M. Pearson, C.-H. Lim, G. M. Miyake, Organocatalyzed Birch reduction driven by visible light. *J. Am. Chem. Soc.* **142**, 13573–13581 (2020).
35. J. Xu, J. Cao, X. Wu, H. Wang, X. Yang, X. Tang, R. W. Toh, R. Zhou, E. K. L. Yeow, J. Wu, Unveiling extreme photoreduction potentials of donor–acceptor cyanoarenes to access aryl radicals from aryl chlorides. *J. Am. Chem. Soc.* **143**, 13266–13273 (2021).
36. S. Wu, J. Kaur, T. A. Karl, X. Tian, J. P. Barham, Synthetic molecular photoelectrochemistry: New frontiers in synthetic applications, mechanistic insights and scalability. *Angew. Chem. Int. Ed.* **61**, e202107811 (2022).
37. C. Monnereau, E. Blart, F. Odobel, A cheap and efficient method for selective para-iodination of aniline derivatives. *Tetrahedron Lett.* **46**, 5421–5423 (2005).
38. L.-G. Xie, D. J. Dixon, Tertiary amine synthesis via reductive coupling of amides with Grignard reagents. *Chem. Sci.* **8**, 7492–7497 (2017).
39. S. Xu, H.-H. Chen, J.-J. Dai, H.-J. Xu, Copper-promoted reductive coupling of aryl iodides with 1,1,1-trifluoro-2-iodoethane. *Org. Lett.* **16**, 2306–2309 (2014).
40. S.-Y. Cheung, H.-F. Chow, T. Ngai, X. Wei, Synthesis of organometallic poly(dendrimer)s by macromonomer polymerization: Effect of dendrimer size and structural rigidity on the polymerization efficiency. *Chem. A Eur. J.* **15**, 2278–2288 (2009).
41. E. Negishi, C. Copéret, S. Ma, T. Mita, T. Sugihara, J. M. Tour, Palladium-catalyzed carbonylative cyclization of 1-iodo-2-alkenylbenzenes. *J. Am. Chem. Soc.* **118**, 5904–5918 (1996).
42. R.-T. Wang, F.-L. Chou, F.-T. Luo, Stereoselective cyclization of (2-bromophenyl)- and (2-iodophenyl)alkynes catalyzed by palladium(O) complexes. *J. Org. Chem.* **55**, 4846–4849 (1990).
43. T. Satoh, K. Itoh, M. Miura, M. Nomura, Desulfonylative iodination of naphthalenesulfonyl chlorides with zinc iodide or potassium-iodide catalyzed by dichlorobis(benzonitrile)palladium(II) in the presence of lithium-chloride and titanium(IV) isopropoxide. *Bull. Chem. Soc. Jpn.* **66**, 2121–2123 (1993).
44. F. De Simone, T. Saget, F. Benfatti, S. Almeida, J. Waser, Formal homo-Nazarov and other cyclization reactions of activated cyclopropanes. *Chem. A Eur. J.* **17**, 14527–14538 (2011).
45. S. G. Newman, V. Aureggi, C. S. Bryan, M. Lautens, Intramolecular cross-coupling of *gem*-dibromoolefins: A mild approach to 2-bromo benzofused heterocycles. *Chem. Commun.* **2009**, 5236–5238 (2009).
46. G. Shi, M. A. Shahid, M. Yousuf, F. Mahmood, L. Rasheed, C. W. Bielawski, K. S. Kim, A "turn-on" fluorescent probe for the detection of permanganate in aqueous media. *Chem. Commun.* **55**, 1470–1473 (2019).
47. Y. Cheng, X. Gu, P. Li, Visible-light photoredox in homolytic aromatic substitution: Direct arylation of arenes with aryl halides. *Org. Lett.* **15**, 2664–2667 (2013).
48. Q. Chen, S. Wu, S. Yan, C. Li, H. Abduhulam, Y. Shi, Y. Dang, C. Cao, Suzuki–Miyaura cross-coupling of sulfoxides. *ACS Catal.* **10**, 8168–8176 (2020).
49. L. Ackermann, H. K. Potukuchi, A. Althammer, R. Born, P. Mayer, Tetra-*ortho*-substituted biaryls through palladium-catalyzed Suzuki–Miyaura couplings with a diaminochlorophosphine ligand. *Org. Lett.* **12**, 1004–1007 (2010).
50. G. Kundu, F. Opincal, T. Sperger, F. Schoenebeck, Air-stable Pd^{I} dimer enabled remote functionalization: Access to fluorinated 1,1-diaryl alkanes with unprecedented speed. *Angew. Chem. Int. Ed. Enlg.* **61**, e202113667 (2022).
51. I. Sapountzis, W. Lin, C. C. Kofink, C. Despotopoulou, P. Knochel, Iron-catalyzed aryl–aryl cross-couplings with magnesium-derived copper reagents. *Angew. Chem. Int. Ed.* **44**, 1654–1658 (2005).
52. R. B. Bedford, N. Fey, M. F. Haddow, R. F. Sankey, Remarkably reactive dihydroindoloindoles *via* palladium-catalysed dearomatisation. *Chem. Commun.* **47**, 3649–3651 (2011).
53. N. Ortega, S. Urban, B. Beiring, F. Glorius, Ruthenium NHC catalyzed highly asymmetric hydrogenation of benzofurans. *Angew. Chem. Int. Ed.* **51**, 1710–1713 (2012).
54. L. Bai, J.-X. Wang, Reusable, polymer-supported, palladium-catalyzed, atom-efficient coupling reaction of aryl halides with sodium tetraphenylborate in water by focused microwave irradiation. *Adv. Synth. Catal.* **350**, 315–320 (2008).
55. K. Dhara, T. Mandal, J. Das, J. Dash, Synthesis of carbazole alkaloids by ring-closing metathesis and ring rearrangement-aromatization. *Angew. Chem. Int. Ed.* **54**, 15831–15835 (2015).
56. C. M. So, H. W. Lee, C. P. Lau, F. Y. Kwong, Palladium-indolylphosphine-catalyzed Hiyama cross-coupling of aryl mesylates. *Org. Lett.* **11**, 317–320 (2009).
57. L. Ackermann, A. R. Kapdi, S. Fenner, C. Kornhaaβ, C. Schulzke, Well-defined air-stable palladium HASPO complexes for efficient Kumada–Corriu cross-couplings of (hetero)aryl or alkenyl tosylates. *Chemistry* **17**, 2965–2971 (2011).

58. M. Amatore, C. Gosmini, Efficient cobalt-catalyzed formation of unsymmetrical biaryl compounds and its application in the synthesis of a sartan intermediate. *Angew. Chem. Int. Ed.* **47**, 2089–2092 (2008).
59. C. Wolf, K. Ekoue-Kovi, Palladium-catalyzed Suzuki–Miyaura cross-coupling using phosphinous acids and dialkyl(chloro)phosphane ligands. *Eur. J. Org. Chem.* **2006**, 1917–1925 (2006).
60. H. W. Lee, F. L. Lam, C. M. So, C. P. Lau, A. S. C. Chan, F. Y. Kwong, Palladium-catalyzed cross-coupling of aryl halides using organotitanium nucleophiles. *Angew. Chem. Int. Ed.* **48**, 7436–7439 (2009).
61. J. M. Antelo Miguez, L. A. Adrio, A. Sousa-Pedrares, J. M. Vila, K. K. Hii, A practical and general synthesis of unsymmetrical terphenyls. *J. Org. Chem.* **72**, 7771–7774 (2007).
62. C.-H. Cho, H. Park, M.-A. Park, T.-Y. Ryoo, Y.-S. Lee, K. Park, Solid-phase synthesis of biphenyls and terphenyls by the traceless multifunctional cleavage of polymer-bound arenesulfonates. *Eur. J. Org. Chem.* **2005**, 3177–3181 (2005).
63. B. Zhou, H. Sato, L. Ilies, E. Nakamura, Iron-catalyzed remote arylation of aliphatic C–H bond via 1,5-hydrogen shift. *ACS Catal.* **8**, 8–11 (2018).
64. A. Mishra, P. Wu, X. Cong, M. Nishiura, G. Luo, Z. Hou, Exo-selective intramolecular C–H alkylation with 1,1-disubstituted alkenes by rare-earth catalysts: Construction of indanes and tetralins with an all-carbon quaternary center. *ACS Catal.* **12**, 12973–12983 (2022).
65. M. Wu, C. Yan, D. Zhuang, R. Yan, Metal-free C–S bond formation in elemental sulfur and cyclobutanol derivatives: The synthesis of substituted thiophenes. *Org. Lett.* **24**, 5309–5313 (2022).
66. A. Kellmann, Intersystem crossing and internal conversion quantum yields of acridine in polar and nonpolar solvents. *J. Phys. Chem.* **81**, 1195–1198 (1977).
67. M. S. Maji, T. Pfeifer, A. Studer, Oxidative homocoupling of aryl, alkenyl, and alkynyl Grignard reagents with TEMPO and dioxygen. *Angew. Chem. Int. Ed.* **47**, 9547–9550 (2008).
68. L. Pause, M. Robert, J.-M. Savéant, Can single-electron transfer break an aromatic carbon-heteroatom bond in one step? A novel example of transition between stepwise and concerted mechanisms in the reduction of aromatic iodides. *J. Am. Chem. Soc.* **121**, 7158–7159 (1999).

Acknowledgments: We thank M. Akita (Tokyo Institute of Technology) and T. Koike (Nippon Institute of Technology) for discussions on a BDA photoredox catalysis. **Funding:** This work has been supported financially in part by JST CREST (JPMJCR18R4). **Author contributions:** Conceptualization: E.S. Data curation: Y.O., K.Y., K.O., S.M., S.K.S., and M.A. Methodology: E.S. Investigation: Y.O., K.Y., K.O., S.M., S.K.S., and M.A. Funding acquisition: E.S. Project administration: E.S. Supervision: E.S., K.Y., and M.A. Writing— original draft: E.S. and K.Y. Writing — review and editing: E.S., K.Y., and M.A. **Competing interests:** The authors declare that they have no competing interests. **Data and materials availability:** All data needed to evaluate the conclusions in the paper are present in the paper and/or the Supplementary Materials.

Submitted 26 February 2023
Accepted 26 April 2023
Published 31 May 2023
10.1126/sciadv.adh3544